ISSN 1674-1056
http://cpb.iphy.ac.cn
http://iopscience.iop.org/cpb
中国物理 B
Chinese Physics
中国物理 Chinese Physics B

Photodynamics of Ga_{Zn}-V_{Zn} complex defect in Ga-doped ZnO

Ai-Hua Tang(汤爱华), Zeng-Xia Mei(梅增霞), Yao-Nan Hou(侯尧楠), Xiao-Long Du(杜小龙)
Citation: Chin. Phys. B . 2018, 27(11): 117802. **doi:** 10.1088/1674-1056/27/117802
Journal homepage: http://cpb.iphy.ac.cn; http://iopscience.iop.org/cpb

What follows is a list of articles you may be interested in

Recent progress on photoluminescence from plasmonic nanostructures: Phenomenon, mechanism, and application

Tingting Yin(尹婷婷), Liyong Jiang(蒋立勇), Zexiang Shen(申泽骧)
Chin. Phys. B . 2018, 27(9): 097803. **doi:** 10.1088/1674-1056/27/9/097803

Transition intensity calculation of Yb: YAG

Hong-Bo Zhang(张洪波), Qing-Li Zhang(张庆礼), Xing Wang(王星), Gui-Hua Sun(孙贵花), Xiao-Fei Wang(王小飞), De-Ming Zhang(张德明), Dun-Lu Sun(孙敦陆)
Chin. Phys. B . 2018, 27(6): 067801. **doi:** 10.1088/1674-1056/27/6/067801

Magneto-optical properties of self-assembled InAs quantum dots for quantum information processing

Jing Tang(唐静), Xiu-Lai Xu(许秀来)
Chin. Phys. B . 2018, 27(2): 027804. **doi:** 10.1088/1674-1056/27/2/027804

Shape controllable synthesis and enhanced upconversion photoluminescence of β-$NaGdF_4$:Yb^{3+}, Er^{3+} nanocrystals by introducing Mg^{2+}

Yong-Xin Yang(杨永馨), Zheng Xu(徐征), Su-Ling Zhao(赵谡玲), Zhi-Qin Liang(梁志琴), Wei Zhu(朱薇), Jun-Jie Zhang(张俊杰)
Chin. Phys. B . 2017, 26(8): 087801. **doi:** 10.1088/1674-1056/26/8/087801

Enhancing redshift phenomenon in time-resolved photoluminescence spectra of AlGaN epilayer

Wei Li(李维), Peng Jin(金鹏), Wei-Ying Wang(王维颖), De-Feng Mao(毛德丰), Xu Pan(潘旭), Xiao-Liang Wang(王晓亮), Zhan-Guo Wang(王占国)
Chin. Phys. B . 2017, 26(7): 077802. **doi:** 10.1088/1674-1056/26/7/077802

Photodynamics of Ga_{Zn}–V_{Zn} complex defect in Ga-doped ZnO*

Ai-Hua Tang(汤爱华)[1,2], Zeng-Xia Mei(梅增霞)[1,†], Yao-Nan Hou(侯尧楠)[1], and Xiao-Long Du(杜小龙)[1,2,‡]

[1] *Key Laboratory for Renewable Energy, Beijing National Laboratory for Condensed Matter Physics, Institute of Physics, Chinese Academy of Sciences, Beijing* 100190, *China*

[2] *School of Physical Sciences, University of Chinese Academy of Sciences, Beijing* 100049, *China*

(Received 22 May 2018; revised manuscript received 2 September 2018; published online 19 October 2018)

The wide-band-gap II–VI compound semiconductor ZnO is regarded as a promising single-photon emission (SPE) host material. In this work, we demonstrate that a $(Ga_{Zn}–V_{Zn})^-$ complex defect can readily be obtained and the density can be controlled in a certain range. In analogy to nitrogen vacancy centers, such a defect in ZnO is expected to be a new single photon source. The optical properties of the $(Ga_{Zn}–V_{Zn})^-$ complex defect are further studied by photoluminescence and time-resolved photoluminescence spectra measurements. The electron transitions between the defect levels emit light at $\sim$ 650 nm with a lifetime of 10–20 nanoseconds, indicating a good coherent length for SPE. Finally, a two-level emitter structure is proposed to explain the carrier dynamics. We believe that the photodynamics study of the $(Ga_{Zn}–V_{Zn})^-$ complex defect in this work is important for ZnO-based quantum emitters.

Keywords: $(Ga_{Zn}–V_{Zn})^-$ complex defect, photoluminescence, time-resolved photoluminescence

PACS: 78.55.–m, 71.55.–I, 78.55.Et, 61.72.J– **DOI:** 10.1088/1674-1056/27/11/117802

1. Introduction

Zinc oxide (ZnO) is a material of practical interest showing significant advantages in several applications including ultraviolet optoelectronic devices, transparent conducting oxide thin films, and spintronics.[1,2] In particular, a wide band gap (3.37 eV at room temperature), large exciton binding energy (60 meV), high electron mobility, visible transparency, and high emission efficiency make ZnO attractive for light-emitting devices.[3] More recently, renewed interest in ZnO has been fueled by its attractive prospects as the host of photonic qubits at room temperature. ZnO has been added to the list of room-temperature single-photon emission (SPE) sources, where it is considered to host defect-related single emitters at room temperature.[4]

The prototypical point-defect qubit is the widely studied nitrogen-vacancy (NV) center in diamond,[5,6] consisting of a nitrogen impurity next to a carbon vacancy, and its crystallographic and electronic structures have been well established.[7,8] Moreover, engineering of two-state defect emitters is necessarily important for device applications. In contrast, point-defect-derived quantum optical applications of ZnO are still in their infancy, since room-temperature SPE has only been reported in recent years.[9–15] Given the lack of reliable experimental data on the point-defect energetics in ZnO, the origin of these luminescent centers is still unclear although it is thought to be related to zinc vacancy (V_{Zn}).[9,13–15] Strikingly, a $(Ga_{Zn}–V_{Zn})^-$ complex defect rather than an isolated V_{Zn}^{2-} was identified as the predominant compensating acceptor center in Ga-doped ZnO via zinc self-diffusion experiments in isotopic heterostructures in our previous work.[16] The study of $(Ga_{Zn}–V_{Zn})^-$-complex-defect–surface-plasmon coupling in this heavily compensated Ga-doped ZnO material has been systematically carried out by optical characterizations[17] based on achieving a high density of controllable $(Ga_{Zn}–V_{Zn})^-$ in Ga-doped ZnO. On the other hand, the photoluminescence characteristics of the $(Ga_{Zn}–V_{Zn})^-$ complex defect itself needs to be explored as it may potentially be a new type of SPE candidate.

In this paper, the energy level structure of $(Ga_{Zn}–V_{Zn})^-$ is first proposed based on photoluminescence spectra (PL) analysis, and the carrier recombination lifetime is obtained from the time-resolved photoluminescence (TRPL) measurements. The electron transitions between the $(Ga_{Zn}–V_{Zn})^-$ complex defect levels emit the light at $\sim$ 650 nm with a lifetime of 10–20 nanoseconds. These findings may be important regarding the structural origin of single-photon emitters in ZnO, which will also advance the applications of $(Ga_{Zn}–V_{Zn})^-$ in single photon sources and high-efficiency nanophotonic emitters.

2. Experiments

The samples were synthesized on sapphire (0001) substrates by radio frequency plasma assisted molecular beam epitaxy (rf-MBE) with a base pressure of $\sim 10^{-10}$ mbar. To obtain high-quality ZnO films, a $\sim$ 20 nm MgO (111) buffer layer was deposited at 773 K on the *c*-oriented sapphire substrate treated with oxygen radicals beforehand. A ZnO buffer

*Project supported by the National Natural Science Foundation of China (Grant Nos. 11674405 and 11675280).

†Corresponding author. E-mail: zxmei@iphy.ac.cn

‡Corresponding author. E-mail: xldu@iphy.ac.cn

© 2018 Chinese Physical Society and IOP Publishing Ltd

layer and epitaxial layer were grown on it successively. More details can be found elsewhere.[16]

An *in situ* reflection high-energy electron diffraction (RHEED) was utilized to monitor the whole epitaxial growth process. The RHEED patterns clearly demonstrated the wurtzite features in all samples during the whole growth process (not shown here). Three samples were prepared, including an intrinsic ZnO (labeled as Z) and two Ga-doped ZnO (labeled as G1 and G2). Ga concentrations in G1 and G2 are $\sim 1\times10^{19}$ cm^{-3} and $\sim 1\times10^{20}$ cm^{-3}, respectively (see Table 1 for an overview of these samples.) It should be noted that the growth limits (Zn and O fluxes) of all samples were kept the same, and the Ga-doped ZnO samples showed a heavily electrical compensation effect. Annealing was performed at 1023 K for 10 min in vacuum. PL spectra were recorded at room temperature by exciting the samples with a 325 nm He–Cd laser with an output power of 136 μW. TRPL measurements were carried out with a 50 ps pulsed laser at an excitation wavelength of 375 nm, and the time resolution is better than 100 ps.

Table 1. Ga concentration and electrical properties of the samples.

Sample	Ga concentration/cm^{-3}	Carrier concentration/cm^{-3}	Mobility/cm$^2\cdot$V$^{-1}\cdot$s^{-1}
G1	$\sim 1\times10^{19}$	-4.96×10^{17}	20.7
G1 AN	$\sim 1\times10^{19}$	-6.75×10^{18}	54.3
G2	$\sim 1\times10^{20}$	-7.37×10^{17}	24.2
Z	–	-1.08×10^{16}	66.0

3. Results and discussion

The room-temperature (RT) PL spectra of the as-grown Ga-doped ZnO samples G1 and G2 are shown in Fig. 1(a). Both samples demonstrate two distinct emission bands: a signature ultraviolet (UV) near-band-edge (NBE) emission of ZnO, and a quite broad visible emission band universally assigned to intrinsic or extrinsic defects, known as deep-level emission (DLE). The near-infrared (NIR) emission peak at $\sim$ 760 nm is a second order of the UV NBE peak. Generally, V_{Zn}-related acceptor defects were assumed to be responsible for the DLE near 650 nm.[18–21] In order to discover the difference between their DLE near 650 nm, the emission intensities of G1 and G2 were normalized at the NBE region, as shown in Fig. 1(a). First of all, the influence of crystal quality on the emission can be reasonably ruled out, because the two samples exhibit almost the same full width at half maximum (FWHM) in x-ray diffraction characterizations (not shown here). Compared with G1, G2 demonstrates a stronger DLE peak at $\sim$ 650 nm, in agreement with the larger compensating acceptor concentration (reflected by the difference between Ga and carrier concentrations in Ga-doped ZnO) in G2 revealed in Table 1.

Figure 1(b) shows the RT PL spectra of the as-grown Ga-doped ZnO sample G1, G1 after annealing at 1023 K in vacuum (G1 AN), and intrinsic ZnO sample Z. Unlike G1, G1 AN and Z show much stronger NBE emission and an obviously weaker blue-shifted DLE peak at $\sim$ 550 nm. It is quite reasonable to attribute the broad PL band at $\sim$ 650 nm to V_{Zn} related defects. As mentioned above, via zinc self-diffusion experiments in isotopic heterostructures, a $(Ga_{Zn}–V_{Zn})^-$ complex defect rather than an isolated V_{Zn}^{2-} has been recognized as the predominant compensating acceptor center in Ga-doped ZnO. Therefore, in the present study, we believe the emission near 650 nm belongs to the two-level emitter of $(Ga_{Zn}–V_{Zn})^-$ instead of a single V_{Zn}, as schematically illustrated in the inset of Fig. 1(b).

As the main acceptor in Ga-doped ZnO, the $(Ga_{Zn}–V_{Zn})^-$ complex defect will dissociate significantly after annealing, resulting in increased conductivity as shown in Table 1. Apparently, the remarkable blue shift of G1's DLE toward the widely studied green band near 550 nm after annealing, shown in Fig. 1(b), should be attributed to the dissociation of substantial $(Ga_{Zn}–V_{Zn})^-$ complex defects. The high density of ionized $(Ga_{Zn}–V_{Zn})^-$ complex defects, contributing to the broad DLE emission at $\sim$ 650 nm, also results in an enhanced nonradiative transition and largely reduced NBE.[22,23] Note that, due to the heavily electrical compensation in our as-grown Ga-doped ZnO samples, the concentrations of free carriers are very low ($\sim 10^{17}$ cm^{-3}),obviously lower than the theoretically calculated critical concentration of the degenerate state for Ga-doped ZnO ($> 10^{18}$ cm^{-3}). Therefore, all as-grown Ga-doped samples are non-degenerate, and the upper level of the $(Ga_{Zn}–V_{Zn})^-$ complex defect will not merge into the conduction band. First, a nonradiative transition happens to the photo-generated electrons from the conduction band to the upper level of the $(Ga_{Zn}–V_{Zn})^-$ complex defect, which is close to the conduction band minimum. Then a large number of electrons transit between the two states of complex defect, causing the intense red DLE at $\sim$ 650 nm. The shallow donor states of isolated Ga_{Zn}^{+} are activated by dissociating the $(Ga_{Zn}–V_{Zn})^-$ complexes, which leads to the band-gap renormalization effect and hence the red shift of NBE.[22]

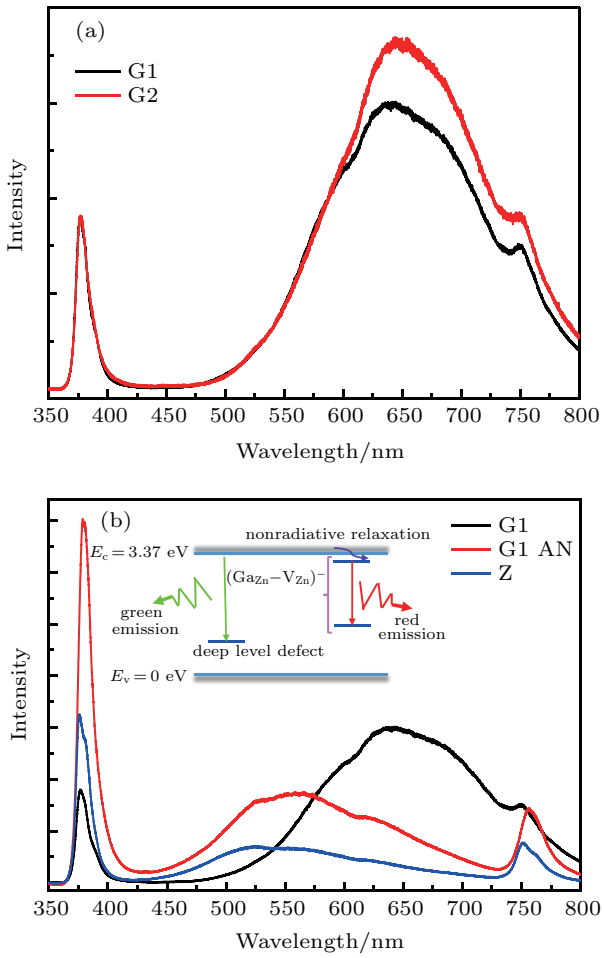


Fig. 1. (color online) (a) Normalized RT PL spectra of G1 and G2. The emission intensities of G1 and G2 were normalized at the NBE region in order to compare the relative intensities of the peaks near 650 nm. (b) RT PL spectra of samples G1, G1 after annealing (G1 AN), and Z. An energy level diagram for DLE is shown in the inset.

Finally, the photodynamic characteristics of $(Ga_{Zn}–V_{Zn})^-$ acceptor complex defects were studied by TRPL spectra. Figure 2 shows the decay profiles of G1, G1 AN, Z, G2, and G2 AN. They were fitted by a triple-exponential function with time constants τ_1, τ_2, and τ_3. The fast decay component τ_1 is commonly attributed to nonradiative recombination,[24] and the slow decay component τ_3 is ascribed to electron communications with the background, which is usually a complex process with a long relaxation time. The remaining component τ_2 (16.46 ns, 15.92 ns, 2.75 ns, 7.24 ns, and 0.78 ns for G1, G2, G1 AN, G2 AN, and Z, respectively) presents the lifetime of the deep level defects. As demonstrated in Fig. 2(a), the decay profile of the visible emission peak of G1 ($\sim$ 650 nm) is obviously different from those of G1 AN and Z ($\sim$ 550 nm). The lifetime of $(Ga_{Zn}–V_{Zn})^-$ complex defect emission is quite longer than that of the green emission. G2 and G2 AN demonstrate the same tendency, as shown in Fig. 2(b). It implies that the involved emission mechanisms are different for the as-grown and annealed samples. As illustrated in Fig. 2(a), the DLE of G1 AN behaves the same as that of Z. The green band emissions of G1 AN and Z are generally ascribed to the transition from the conduction band to the deep defect level, which was attributed to a single positively charged oxygen vacancy (V_O^+) in previous work.[18,25,26] The results indicate that the initial state of $(Ga_{Zn}–V_{Zn})^-$ complex defect emission is not the conduction band, further confirming the two-level emitter model of the $(Ga_{Zn}–V_{Zn})^-$ complex defect. Consequently, the recombination of electrons between the $(Ga_{Zn}–V_{Zn})^-$ complex defect levels emits light centered at 650 nm with a lifetime of 10–20 nanoseconds, which is closed to the reported lifetime of SPE in ZnO film.[9]

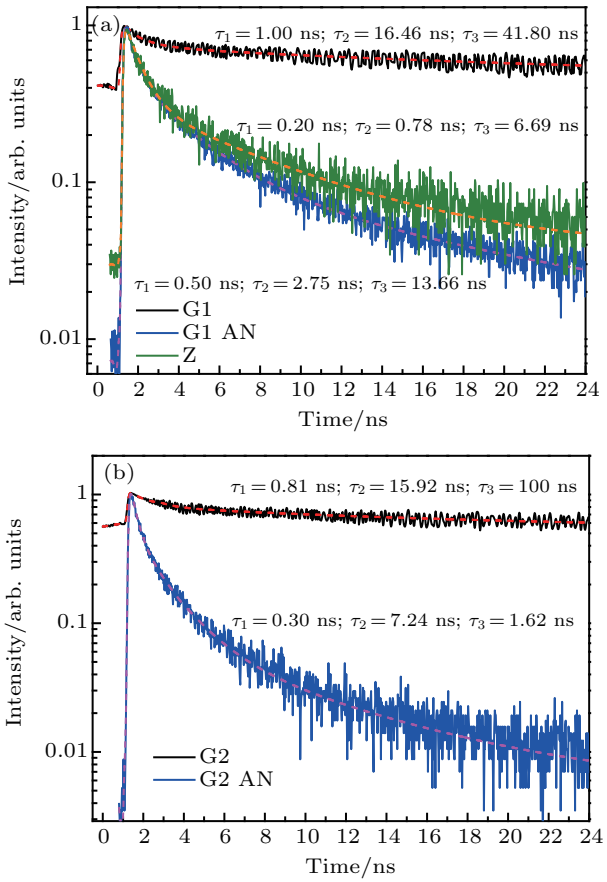


Fig. 2. (color online) Decay profiles and their fitting curves of the center wavelength of the visible emission peaks of (a) G1 ($\sim$ 650 nm), G1 AN ($\sim$ 550 nm), Z ($\sim$ 550 nm), (b) G2 ($\sim$ 650 nm) and G2 AN ($\sim$ 550 nm), respectively.

4. Conclusion and perspectives

The energy level structure of $(Ga_{Zn}–V_{Zn})^-$ was proposed based on the PL spectra, and the lifetime was obtained from the TRPL measurements. The electron transitions between the $(Ga_{Zn}–V_{Zn})^-$ complex defect levels emit light at $\sim$ 650 nm with a lifetime of 10–20 nanoseconds. These findings may advance the exploration of its new applications in single photon sources and high-efficiency nanophotonic emitters.

References

[1] Özgür Ü Alivov Y I, Liu C, Teke A, Reshchikov M A, Doğan S, Avrutin V, Cho S J and Morkoç H 2005 *J. Appl. Phys.* **98** 041301

[2] Pan F, Song C, Liu X J, Yang Y C and Zeng F 2008 *Mater. Sci. Eng. R Rep.* **62** 1
[3] Chu S, Wang G, Zhou W H, Lin Y Q, Chernyak L, Zhao J Z, Kong J Y, Li L, Ren J J and Liu J L 2011 *Nat. Nanotechnol.* **6** 506
[4] Aharonovich I, Englund D and Toth M 2016 *Nat. Photon.* **10** 631
[5] Kurtsiefer C, Mayer S, Zarda P and Weinfurter H 2000 *Phys. Rev. Lett.* **85** 290
[6] Doherty M W, Manson N B, Delaney P, Jelezko F, Wrachtrup J and Hollenberg L C L 2013 *Phys. Rep.* **528** 1
[7] Manson N B, Harrison J P and Sellars M J 2006 *Phys. Rev. B* **74** 104303
[8] Gali A, Fyta M and Kaxiras E 2008 *Phys. Rev. B* **77** 155206
[9] Jungwirth N R, Pai Y Y, Chang H S, MacQuarrie E R, Nguyen K X and Fuchs G D 2014 *J. Appl. Phys.* **116** 043509
[10] Chung K, Karle T J, Khalid A, Abraham A N, Shukla R, Gibson B C, Simpson D A, Djurišic A B, Amekura H and Tomljenovic-Hanic S 2017 *Nanophotonics* **6** 269
[11] Jungwirth N R, Chang H S, Jiang M and Fuchs G D 2016 *ACS Nano* **10** 1210
[12] Choi S, Berhane A M, Gentle A, Ton-That C, Phillips M R and Aharonovich I 2015 *ACS Appl. Mater. Interfaces* **7** 5619
[13] Neitzke O, Morfa A, Wolters J, Schell A W, Kewes G and Benson O 2015 *Nano Lett.* **15** 3024
[14] Choi S, Johnson B C, Castelletto S, Ton-That C, Phillips M R and Aharonovich I 2014 *Appl. Phys. Lett.* **104** 261101
[15] Morfa A J, Gibson B C, Karg M, Karle T J, Greentree A D, Mulvaney P and Tomljenovic-Hanic S 2012 *Nano Lett.* **12** 949
[16] Tang A H, Mei Z X, Hou Y N, Liu L S, Venkatachalapathy V, Azarov A, Kuznetsov A and Du X L 2018 *Sci. Chin. Phys. Mech. Astron.* **61** 077311
[17] Hou Y N, Mei Z X, Tang A H, Liang H L and Du X L 2018 *Phys. Status Solidi A* **215** 1800037
[18] Zeng H B, Duan G T, Li Y, Yang S K, Xu X X and Cai W P 2010 *Adv. Funct. Mater.* **20** 561
[19] Wang X J, Vlasenko L S, Pearton S J, Chen W M and Buyanova I A 2009 *J. Phys. Appl. Phys.* **42** 175411
[20] Look D C, Leedy K D, Vines L, Svensson B G, Zubiaga A, Tuomisto F, Doutt D R and Brillson L J 2011 *Phys. Rev. B* **84** 115202
[21] Dong Y, Tuomisto F, Svensson B G, Kuznetsov A Y and Brillson L J 2010 *Phys. Rev. B* **81** 081201(R)
[22] Ye J D, Gu S L, Zhu S M, Liu S M, Zheng Y D, Zhang R and Shi Y 2005 *Appl. Phys. Lett.* **86** 192111
[23] Tsang J C, Dean P J and Landsberg P T 1968 *Phys. Rev.* **173** 814
[24] Huang X H, Chen R, Zhang C, Chai J W, Wang S J, Chi D Z and Chua S J 2016 *Adv. Opt. Mater.* **4** 960
[25] Wu X L, Siu G G, Fu C L and Ong H C 2001 *Appl. Phys. Lett.* **78** 2285
[26] Ton-That C, Weston L and Phillips M R 2012 *Phys. Rev. B* **86** 115205